



Transseptal puncture in left atrial appendage closure guided by 3D printing and multiplanar CT reconstruction

Marek Hozman MD¹  | Dalibor Herman MD, PhD¹ | David Zemanek MD, PhD² | Ondrej Fiser MSc, PhD³ | David Vrba MSc, PhD³ | Martin Poloczek MD⁴ | Ivo Varvarovsky MD, PhD⁵ | Peter Obona MD⁶ | Tomas Pokorny MSc³ | Pavel Osmancik MD, PhD¹ 

¹Cardiocenter, Third Faculty of Medicine, University Hospital Kralovske Vinohrady, Charles University, Prague, Czech Republic

²Second Department of Internal Medicine, Charles University, Prague, Czech Republic

³Department of Biomedical Technology, Faculty of Biomedical Engineering, CTU in Prague, Prague, Czech Republic

⁴Department of Internal Medicine and Cardiology, University Hospital Brno and Faculty of Medicine of Masaryk University, Brno, Czech Republic

⁵Cardiology Center AGEL, Pardubice, Czech Republic

⁶Cardiocenter, University Hospital Nitra, Nitra, Slovakia

Correspondence

Marek Hozman, MD, Cardiocenter, Third Faculty of Medicine, University Hospital Kralovske Vinohrady, Charles University, Srobarova 1150/50, Prague 100 34, Czech Republic.
Email: hozmanm@gmail.com

Funding information

National Institute for Research of Metabolic and Cardiovascular Diseases, Grant/Award Number: ID Project No. LX22NPO5104; European Union—Next Generation EU; Charles University Research Program “Cooperatio Cardiovascular Sciences”

Abstract

Background: The presented study investigates the application of bi-arterial 3D printed models to guide transseptal puncture (TSP) in left atrial appendage closure (LAAC).

Aims: The objectives are to (1) test the feasibility of 3D printing (3DP) for TSP guidance, (2) analyse the distribution of the optimal TSP locations, and (3) define a CT-derived 2D parameter suitable for predicting the optimal TSP locations.

Methods: Preprocedural planning included multiplanar CT reconstruction, 3D segmentation, and 3DP. TSP was preprocedurally simulated in vitro at six defined sites. Based on the position of the sheath, TSP sites were classified as optimal, suboptimal, or nonoptimal. The aim was to target the TSP in the recommended position during the procedure. Procedure progress was assessed post hoc by the operator.

Results: Of 68 screened patients, 60 patients in five centers (mean age of 74.68 ± 7.64 years, 71.66% males) were prospectively analyzed (3DP failed in one case, and seven patients did not finally undergo the procedure). In 55 patients (91.66%), TSP was performed in the optimal location as recommended by the 3DP. The optimal locations for TSP were postero-inferior in 45.3%, mid-inferior in 45.3%, and antero-inferior in 37.7%, with a mean number of optimal segments of 1.34 ± 0.51 per patient. When the optimal TSP location was achieved, the procedure was considered difficult in only two (3.6%) patients (but in both due to complicated LAA anatomy). Comparing anterior versus posterior TSP in 2D CCT, two parameters differed significantly: (1) the angle supplementary to the LAA ostium and the interatrial septum angle ($160.83^\circ \pm 9.42^\circ$ vs. $146.49^\circ \pm 8.67^\circ$; $p = 0.001$), and (2) the angle between the LAA ostium and the mitral annulus ($95.02^\circ \pm 3.73^\circ$ vs. $107.38^\circ \pm 6.76^\circ$; $p < 0.001$), both in the sagittal plane.

Abbreviations: 2D, two-dimensional; 3D, three-dimensional; 3DP, three-dimensional printing; AF, atrial fibrillation; CCT, cardiac computed tomography; CT, computed tomography; DICOM, Digital Imaging and COmmunications in Medicine; DOAC, direct anticoagulant; FO, fossa ovalis; IAS, interatrial septum; ICE, intracardiac echocardiography; LA, left atrium; LAA, left atrial appendage; LAAC, left atrial appendage closure; LIPV, left inferior pulmonary vein; LMWH, low molecular weight heparin; LSPV, left superior pulmonary vein; LV, left ventricle; LZ, landing zone; TOE, transoesophageal echocardiography; TSP, transseptal puncture; VKA, vitamin K antagonist; VR, virtual reality.

This is an open access article under the terms of the Creative Commons Attribution-NonCommercial-NoDerivs License, which permits use and distribution in any medium, provided the original work is properly cited, the use is non-commercial and no modifications or adaptations are made.

© 2023 The Authors. *Catheterization and Cardiovascular Interventions* published by Wiley Periodicals LLC.

Conclusions: In vitro TSP simulation accurately determined the optimal TSP locations for LAAC and facilitated the procedure. More than one-third of the optimal TSP sites were anterior.

KEYWORDS

3D printing, computed tomography, left atrial appendage closure, transeptal puncture

1 | INTRODUCTION

Affecting 2%–4% of the world's population, atrial fibrillation (AF) is the most common sustained cardiac arrhythmia in adults.¹ It is associated with higher mortality² and a three- to fivefold increase in the risk of stroke.³ In addition, AF-related strokes are more disabling than noncardioembolic strokes.⁴ Echocardiographic and autopsy evidence suggests that up to 90% of left atrial thrombi originate from the left atrial appendage.⁵

Left atrial appendage closure (LAAC) was developed as a nonpharmacological approach to stroke prevention in patients contraindicated to anticoagulation. Two randomized control trials (PROTECT AF, PREVAIL) have corroborated the noninferiority of LAAC to warfarin for preventing ischaemic stroke in nonvalvular atrial fibrillation.^{6,7} More recently, the PRAGUE-17 randomized control trial has demonstrated the noninferiority of LAAC to direct anticoagulants (DOACs) for the prevention of net ischaemic/bleeding events in high-risk populations.⁸

Interindividual variability in the left atrial appendage (LAA) anatomy (varying in the number of lobes, orientation, width, and length) can hinder adequate LAAC device placement. As a result, the procedure could be prolonged, repeated recaptures may occur, or even new transeptal punctures may be necessary; thus, ultimately increasing the risk of periprocedural complications (4.5% cases with procedural complications in the PREVAIL trial).⁷ Careful preprocedural planning is essential to address the issue. In 2015, 3-dimensional printing (3DP) appeared in the reference literature as one of the conventionally available modalities such as 2- and 3-dimensional (2D and 3D) transoesophageal echocardiography (TOE) and cardiac computed tomography (CCT).⁹

To date, 3DP has only been studied for device sizing—one of the critical moments in preprocedural imaging.¹⁰ The transeptal puncture (TSP) location constitutes another crucial procedure element. In general, it is recommended to perform the TSP posteriorly and inferiorly. However, an anterior TSP may be required in patients with a lateral or posterior orientation of the left atrial appendage.¹¹ Therefore, careful preprocedural planning of the TSP using the 3D-printed atrial models could be advantageous. It could allow testing of different TSP locations with actual delivery sheaths and assess the coaxiality of the sheath with the LAA axis from different TSP locations. However, creating a complex bi-atrial model is technically more challenging, possibly due to a lack of evidence in this particular field.

The objectives of the present project are to: (1) evaluate the feasibility of 3D printing for the TSP guidance, (2) analyse the optimal

TSP location distribution, and (3) define a computed-tomography-derived (CT) 2D parameter suitable for predicting optimal TSP positions.

2 | METHODS

2.1 | Study design

The present article is based on a prospective cohort study. All consecutive patients scheduled for LAAC at the five participating centers were screened from February 2021 to March 2023 (initially, only one center participated; the others joined later). Patients were included in the study if they met the following criteria: age over 18 years, ability to grant informed consent, and indication for LAAC procedure according to current guidelines. Exclusion criteria were as follows: LAA thrombus, inadequate CCT or subsequent 3DP quality, severe renal impairment (glomerular filtration rate below 30 mL/min/1.73 mL²) and other individual contraindications (listed below). Before the procedure, each subject underwent a CCT followed by 3DP. As part of the preprocedure planning, a bi-atrial 3DP model was used to simulate the in vitro TSP. Based on the simulation results, the optimal TSP site(s) to be targeted was communicated to the physician performing the procedure.

The operator was briefed on the optimal TSP results and attempted to perform TSP at the recommended location using intraprocedural intracardiac echocardiography (ICE) or TOE navigation. Consecutively, the operator and the echocardiographer assessed the correlation between the recommended and actual TSP locations and the procedure course. The study was approved by the respective ethics committees of all participating centers, and all patients signed an informed consent form before enrollment. The study protocol was published on the clinicaltrials.gov website (NCT05743322).

2.2 | CT scan acquisition

CCT was performed 7–30 days before the procedure commencement. All centers used the same standardized imaging protocol. A Siemens Drive 2 × 128-series CT scanner (Siemens Healthineers) was used in our facility. The technical parameters were as follows: tube voltage 100 kV, tube reference current 230 mA using CARE Dose 4D (automatic exposure control), collimation 128 × 0.62 mm, pitch 0.17, and slice thickness 0.6 mm. The CCT scans were performed in an

out-patient clinic; therefore, no intravenous fluids were administered before data acquisition.

Three phases of contrast agent injection totaling 80 mL (Iomeron, Bracco Imaging) were administered: (1) 60 mL at a flow rate of 4.0 mL/s, (2) 40 mL of a 25% mixture of contrast agent and saline at a flow rate of 4.0 mL/s, and (3) a flush of 30 mL of saline at a flow rate of 4.0 mL/s. Automatic bolus monitoring was initiated at 100 Hounsfield units. Retrospective electrocardiographic gating was used with image reconstruction typically during end-diastole (at ~70% of the R-R interval).

2.3 | Multiplanar CT reconstruction

CCT images were analyzed using FluoroCT 3.2 for OS X 10.11 (the application was developed by P. Theriault-Lauzier). Multiplanar reconstructions were performed to acquire the following parameters: LAA ostium, landing zone (LZ), and ovality index. The LAA ostium area was measured in the plane intersecting the circumflex artery and the tip of the coumadin ridge. The LZ was measured 10 mm distal to the ostium plane using Amulet devices (Abbott Vascular). For the procedures performed with the Watchman device (Boston Scientific), the LZ was measured in the plane intersecting the circumflex artery and a superior point 10–20 mm deeper in the LAA. In addition, three other parameters were measured: (1) the angle between the LAA ostium and the line intersecting the two mitral valve hinge points in the sagittal plane (similar to the apical two-chamber echocardiographic projection), (2) the angle complementary to that between the LAA ostium and the interatrial septum (IAS) in the sagittal plane, and (3) in the frontal plane.

2.4 | Segmentation and 3D printing

Based on CCT data stored in the standardized Digital Imaging and Communications in Medicine (DICOM) format, segmentation was performed using Mimics 24.0 and 3-Matic 16.0 software (Materialise) or 3D Slicer 4.11.20210226 (The Slicer Community, www.slicer.org). In terms of the segmentation method, automatic boundary detection

followed by manual correction (often necessary for the right atrium) was applied in most cases. Only a few models were segmented solely by manual delineation (right atrium only), which could be performed by an experienced technician or physician in ~30 min (after a practice run of 10 segmentations). Each model comprised both atria with adjacent portions of the pulmonary veins and the superior and inferior vena cava (Figure 1). A wall thickness of 3 mm was typically set to preserve model integrity. The model was exported in stereolithography (STL) format and then printed using the Original Prusa i3 MK3S 3D printer and Flexfill 98A elastic filament (Prusa Research). The filament printer was chosen because it allows the production of more extensive modes than resin printers. Each model's dimensions were manually cross-checked by measuring various anatomical reference points (pulmonary vein ostia, tricuspid, and mitral annuli, the distance between the tips of both appendages) and correlated with the CCT to ensure an accurate 1:1 representation of the CCT data. The average production time for the 3D-printed model was 8–12 h.

2.5 | In vitro simulation

Before each procedure, in vitro TSP puncture was simulated using 3DP models as part of preoperative planning. The original 12 Fr delivery sheath (Abbott) was used to do so. Initially, six holes (TSP locations) were drilled through the IAS from the right side of the septum using a cordless drill. In some cases, small portions of the right atrium had to be dissected to gain optimal access to the IAS. The puncture sites were placed as follows: three in the cranial part of the fossa ovalis (FO) (anteriorly [just behind the aortic root], centrally and posteriorly) and three in the caudal part of the FO in the same manner (anterior, central, and posterior). For optimal visualization of the proximal LAA segment, a portion of the LA was cut just proximal to the LAA ostium as well as the right-sided pulmonary veins (to visualize the LAA ostium “en face”). The delivery sheath was inserted through all six preformed holes, and its distal end was placed into the LAA (10–20 mm deep). The relationship between the sheath and the proximal segment of the LAA was evaluated in two orthogonal views. For the puncture site to be considered optimal, two

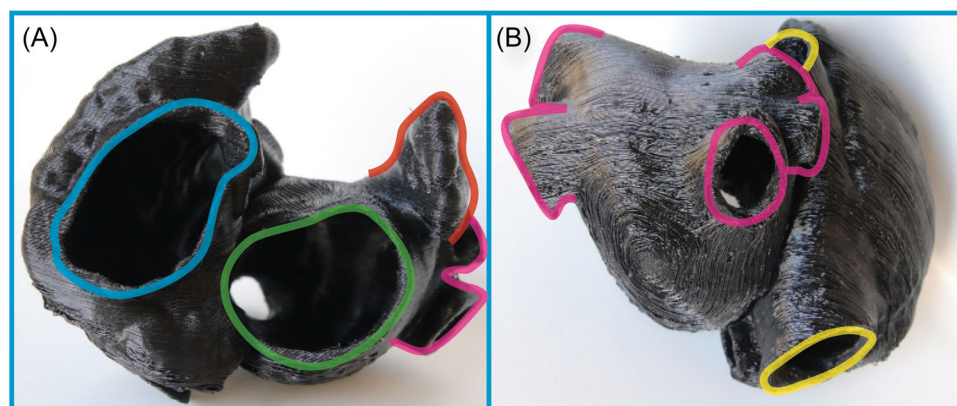


FIGURE 1 3D-printed model. (A) Anterior view, (B) posterior view; blue, tricuspid annulus; green, mitral annulus; pink, pulmonary veins; red, left atrial appendage; yellow, superior vena cava, and inferior vena cava. [Color figure can be viewed at wileyonlinelibrary.com]

criteria had to be met in both views: (1) a central sheath position (in the LAA ostium), and (2) a coaxial sheath position (i.e., an angle between the sheath and the LAA ostium axis not exceeding 30°). If only one or none of the criteria were met in both views, the position was designated suboptimal or nonoptimal, respectively (Figure 2).

2.6 | Landing zone measurements

The present study intended to assess the utility of 3D printing for TSP, not for device sizing. The 3D models were not used for landing zone measurement in any patient; LZs were measured by TOE, CT, or angiography. However, the final device selection was at the discretion of the operator.

During TOE, the LZ was measured in different mid-oesophageal views (~45°–135°). A maximum endocardial distance of ~10 mm distal to the LAA ostium was obtained during mid-diastole.

The mean LZ diameter was calculated as part of the CCT analysis using the LAA perimeter, measured in a plane depending on the device type (see above).

Angiographic measurements were obtained after TSP with a pigtail catheter placed in the LAA. A 12 or 14 Fr delivery sheath was used for calibration. At least two angiographic projections were taken (right anterior oblique 30° + cranial 10°–20° and caudal 10°–20°), measuring the maximum values.

2.7 | Procedure

Experienced operators performed all procedures according to the current guidelines.¹¹ ICE intraprocedural imaging was used in one

center, whereas in the other facilities, the procedures were guided by TOE. Before the procedure, each operator received a recommendation for the optimal puncture site based on the results of the *in vitro* simulation. In ICE-guided cases, the actual puncture site was classified as posterior (toward the left-sided pulmonary veins), anterior (toward the LAA), or middle (between the previous and toward the coumadin ridge) based on the LA anatomic structures visible during the TSP in the projection plane (Figure 3). In TOE-guided procedures, short-axis views of the mid-esophageal aortic valve (~25°–45°) and mid-esophageal bicaval views (~90°–110°) were mainly used. Depending on the IAS third where the puncture was performed, it was categorized as anterior, medial, or posterior (short axis view of the aortic valve). The craniocaudal localization was shown in the bicaval projection.

Each procedure course was rated by the performing physician as easy or difficult (according to the operator's satisfaction with LAA intubation after TSP, the coaxiality of the delivery sheath with the appendage, and the ease of the occluder delivery in the correct position relative to the TSP).

3DP models were not used to determine device sizing; it was done based on CCT and TOE data and intraprocedural angiography according to the preference of the performing physicians.

2.8 | Statistical analysis

The data collected were analyzed using SPSS Statistics 25 software (IBM Corporation). The Shapiro–Wilk test of normality was applied to assess the normal distribution of continuous variables. The Whitney–Mann *U* test or the Student *t* test was applied to compare the continuous

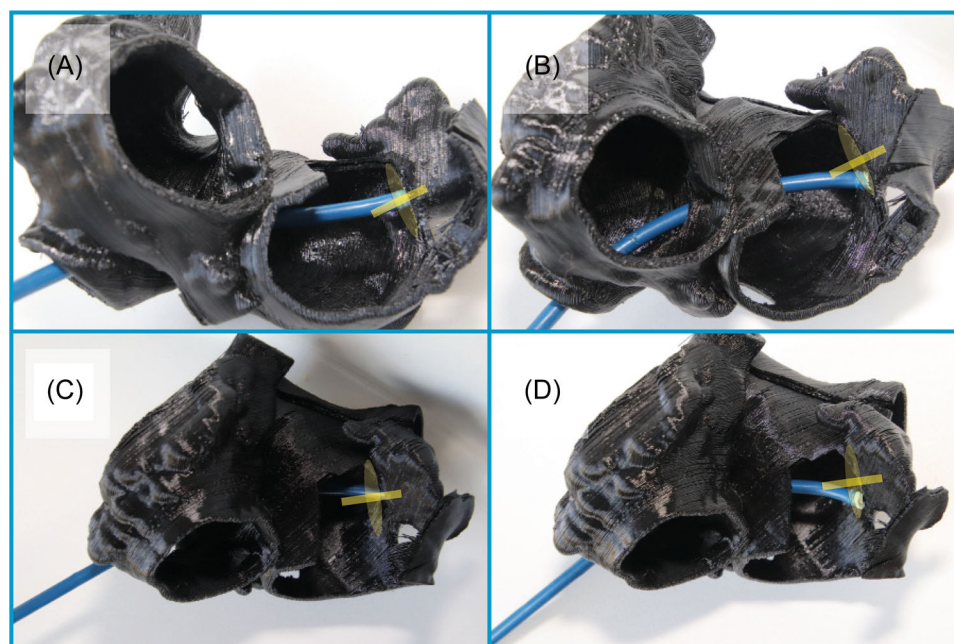


FIGURE 2 In vitro TSP simulation. LAA ostium and its axis are marked in yellow; (A and B) left anterior oblique (LAO) projection, (C and D) LAO with cranial angulation; (A and C) optimal sheath position (posterior TSP), (B and D) nonoptimal sheath position (anterior TSP). LAO, left anterior oblique; TSP, transseptal puncture. [Color figure can be viewed at [wileyonlinelibrary.com](https://onlinelibrary.wiley.com/doi/10.1111/j.1522-2666.2023.02372.x)]

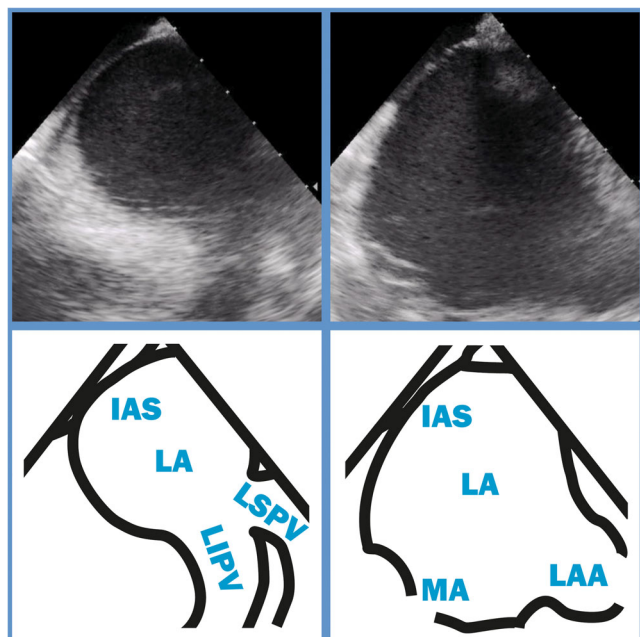


FIGURE 3 ICE images with explanatory notes (posterior plane left and anterior plane right); IAS, interatrial septum; LA, left atrium; LAA, left atrial appendage; LIPV, left inferior pulmonary vein; LSPV, left superior pulmonary vein; MA, mitral annulus. [Color figure can be viewed at [wileyonlinelibrary.com](https://onlinelibrary.wiley.com)]

variables between the two groups. Pearson correlation and paired *t* test were used to analyse the relationship between different LZ measurement methods. All tests were two-tailed and were performed at a 5% significance level.

3 | RESULTS

3.1 | Patient population and preoperative assessment

Altogether, 68 patients scheduled for LAAC were screened. Eight of them were excluded: 3DP had failed in one case, and the remaining seven patients did not undergo the procedure for a variety of reasons (one patient died before the procedure, one had contraindications due to liver cirrhosis, one patient sustained severe trauma before the procedure, and four patients were diagnosed with LAA thrombus). The study, therefore, included a cohort of 60 patients.

The majority of the cohort was male (71.66%), with a mean age of 74.68 (± 7.64) years. The most prevalent contraindication to anticoagulation was intracranial haemorrhage (42.3%), followed by gastrointestinal bleeding (22.0%). Baseline characteristics are detailed in Table 1. A model could not be constructed in one case (1.5%) due to poor quality CCT. The remaining patients encountered no significant problems with the segmentation or the printing process.

TABLE 1 Baseline characteristics of the study cohort.

Characteristic	All patients (N = 60)
Gender	
Male (%)	43 (71.66)
Female (%)	17 (28.34)
Age, mean (years)	74.68 \pm 7.64
Body mass index, mean (kg/m ²)	28.34 \pm 5.06
<i>Coexisting disease</i>	
Nonpermanent atrial fibrillation (%)	35 (58.33)
Permanent atrial fibrillation (%)	25 (41.67)
Heart failure (%)	14 (23.33)
Ischemic heart disease (%)	21 (35.00)
Diabetes mellitus (%)	9 (15.00)
History of ischemic stroke (%)	23 (38.33)
History of intracranial haemorrhage (%)	26 (43.33)
CHA ₂ DS ₂ -VASc score	3.85 \pm 1.38
HAS-BLED score	3.11 \pm 1.10
<i>Antithrombotic medication</i>	
VKA (%)	4 (6.67)
DOAC (%)	7 (11.67)
Reduced DOAC (%)	11 (18.33)
LMWH (%)	16 (26.67)
Aspirin (%)	6 (10.00)
Clopidogrel (%)	10 (16.67)
None (%)	6 (10.00)

Note: Data expressed as means \pm standard deviation or number of patients (percentages).

Abbreviations: DOAC, direct anticoagulant (apixaban, dabigatran, rivaroxaban); LMWH, low molecular weight heparin; LV, left ventricle; VKA, vitamin K antagonist.

3.2 | Procedural characteristics

In 55 cases (91.66%), TSP was performed at the optimal site according to the recommendations of the preprocedural 3DP simulation in vitro (54.54% ICE-guided and 55.46% TOE-guided). Operators rated only two (3.63%) of the 55 procedures as difficult (in both cases, the difficulties were caused not by a misalignment of the sheath with the LAA axis but by unusual LAA morphology). Device recapture was reported in three cases (5.45%), all due to the need for resizing. The Amulet device was most frequently involved (55 cases, 91.66%).

The TSP was performed in five cases (8.33%) at other than the optimal location as recommended by the 3DP. The operator classified the procedure as difficult in four cases (80%) due to the nonoptimal position of the sheath relative to the LAA axis. Despite the

TABLE 2 Procedural characteristics.

Characteristic	All patients (N = 60)
Mean procedural time (min)	85.42 (± 15.97)
Mean fluoroscopic time (min)	10.07 (± 3.04)
Optimal in vivo TSP location	55 (91.66)
Sub- or nonoptimal in vivo TSP location	5 (8.33)
Device recapture	3 (5.45)
Amulet device	55 (91.66)
Watchman device	5 (8.33)

Note: Data are expressed as mean ± standard deviation or number of patients (%).

Abbreviation: TSP, transeptal puncture.

nonoptimal angle between the sheath and the LAA axis, the LAA was eventually closed in all four patients. No device recapture or procedure-related complications were observed in this group. The procedural characteristics are summarized in Table 2.

3.3 | Optimal distribution of puncture sites

In procedures rated as easy by the operator, distribution of optimal puncture sites was analyzed. To this end, five patients were excluded because the actual puncture was performed in a nonoptimal section of the FO (based on the 3DP simulation) and two patients were excluded because the TSP was performed in the recommended sites, but the operator judged the progression of the procedure to be difficult. Thus, 53 patients entered the analysis. The most frequent optimal TSP sites were postero-inferior and mid-inferior (45.28% for both sites) and antero-inferior (37.73%). The superior TSP sites were optimal in only 9.43% of cases. Notably, the adjacent inferior site was also optimal in all these patients. The mean number of optimal TSP sites per patient was 1.34 (±0.51), with 18 (34.00%) patients having two or more optimal segments. The distribution of optimal puncture sites is shown in Figure 4.

3.4 | Two-dimensional characteristics of the optimal TSP

As mentioned above, the anterior TSP was considered optimal in 37.7% of patients. To compare parameters on 2D CCT related to posterior versus anterior TSP, the angles between the LAA ostium, IAS, and mitral annulus were measured on 2D CCT in 53 patients (described above). The analysis aimed to identify parameters that could be easily measured on 2D CCT and were suitable for TSP guidance (anterior or posterior), avoiding using 3DP.

When comparing patients with anterior-only optimal puncture sites and those with posterior-only optimal puncture sites, the angle between the LAA ostium and the mitral annulus (mean 95.02° ± 3.73°

Optimal puncture sites

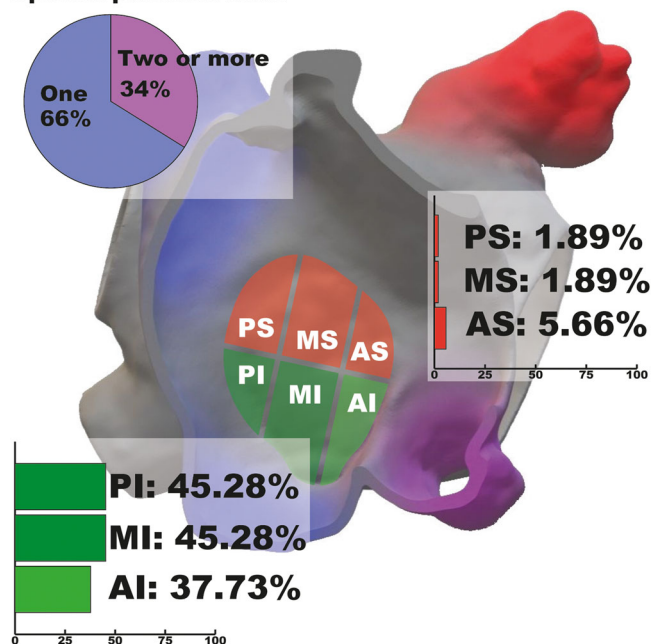


FIGURE 4 3D segmentation (lateral right atrium cut off), interatrial septum (RAO view) with TSP locations. AI, antero-inferior. Graphs indicate the prevalence of more than one optimal TSP site per patient and the frequencies of optimal locations for each site (superior positions are marked in red, and inferior are marked in green). AI, antero-inferior; AS, antero-superior; Blue, superior and inferior venae cavae; MI, mid-inferior; MS, mid-superior; PI, postero-inferior; PS, postero-superior; purple, coronary sinus; red, LAA. [Color figure can be viewed at wileyonlinelibrary.com]

vs. 107.38° ± 6.76°; $p < 0.001$) (Figures 5 and 6) and the angle between the LAA ostium and the IAS in the sagittal plane (mean 160.83° ± 9.42° vs. 146.49° ± 8.67°; $p = 0.001$) differed significantly. Conversely, there were no significant differences in the angle between the LAA ostium and the IAS in the frontal plane (mean 120.21° ± 16.65° vs. 124.02° ± 9.60°; $p = 0.22$).

3.5 | Peri-procedural complications

In two cases, cardiac tamponade occurred after device insertion. Surgical revision was required in one case. The procedure was considered straightforward, and the device was implanted on the first deployment. The tamponade was probably attributable to the anchor hooks of the device in frail patients. The second procedure, complicated by tamponade, was difficult due to unusual LAA anatomy and incorrect LZ measurement requiring reinsertion of the device more than 10 times. Fortunately, the bleeding stopped after pericardiocentesis. One patient, categorized as a straightforward procedure, experienced device embolisation into the descending aorta within 24 h of the procedure due to incorrect sizing. In all three cases mentioned, the TSPs were performed in optimal locations.

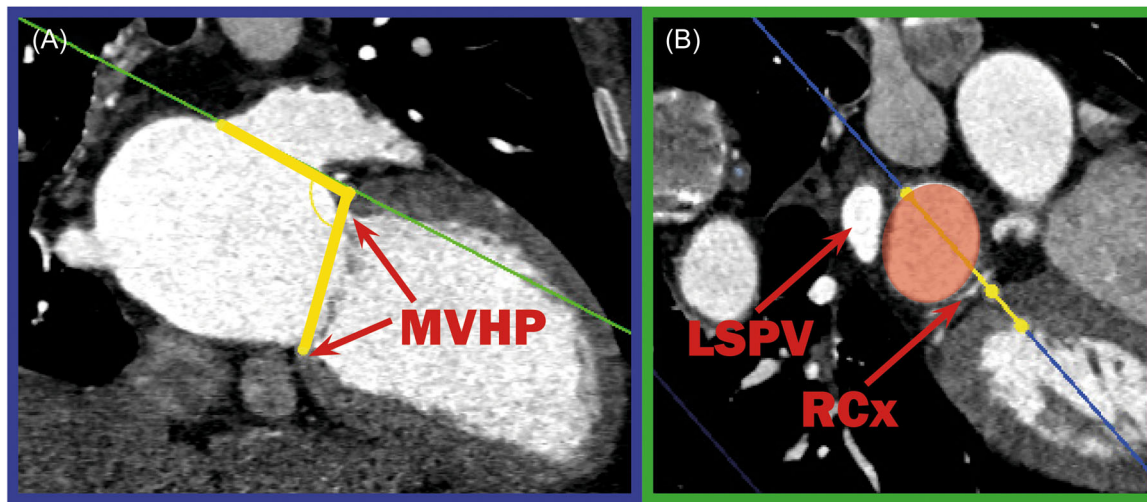


FIGURE 5 Measurement of the angle between the LAA ostium and the mitral annulus; two orthogonal planes are depicted. (A) Two chamber sagittal plane, green line displays the plane B, the angle between the LAA ostium and the mitral annulus marked in yellow; (B) an orthogonal plane at the level of the LAA ostium, blue line displays the plane A, the LAA ostium is marked in red. LSPV, left superior pulmonary vein; MVHP, mitral valve hinge points; RCx, circumflex artery. [Color figure can be viewed at [wileyonlinelibrary.com](https://onlinelibrary.com)]]

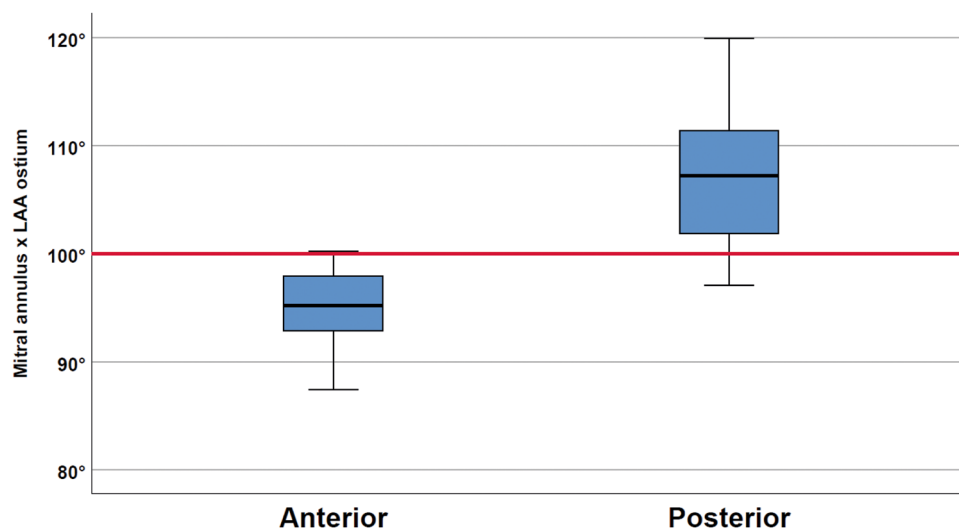


FIGURE 6 Boxplot comparing anterior and posterior optimal locations (LAA ostium × mitral annulus angle in the y-axis), the value 100° is marked in red. LAA, left atrial appendage closure. [Color figure can be viewed at [wileyonlinelibrary.com](https://onlinelibrary.com)]]

3.6 | Landing zone measurements

In 40 (60%) cases, LZ measurements were recorded using all three modalities (angiography, TOE, and CCT). A statistically significant linear correlation between them was observed: $R = 0.55$ ($p < 0.001$) for angiography versus TOE, $R = 0.63$ ($p < 0.001$) for angiography versus CCT and $R = 0.56$ ($p < 0.001$) for TOE versus CCT. However, the mean values were significantly different in all three comparisons: angiography versus TOE $p = 0.044$ (95% CI 0.03–2.22), angiography versus CCT $p < 0.001$ (95% CI –4.76 to –2.62), and TOE versus CCT $p < 0.001$ (95% CI –5.99 to –3.65). The most significant measured values were obtained with CCT (mean 23.35 ± 4.20 mm), followed by angiography (mean 19.66 ± 3.40 mm) and TOE (mean 18.53 ± 3.80 mm). Bland–Altman plots

are shown in Figure 7. As mentioned above, 3D-printed models were not used for LZ measurements.

4 | DISCUSSION

This prospective study shows that the biatrial 3DP model can be easily produced for most LAAC-scheduled patients. For 92% of the patients, the TSP could be performed according to the preprocedural 3DP recommendation. The procedure was uncomplicated regarding the course of the delivery sheath with the LAA in 96% of patients treated according to the 3DP recommendation. The most recommended optimal TSP locations were postero-inferior and mid-inferior (45% for

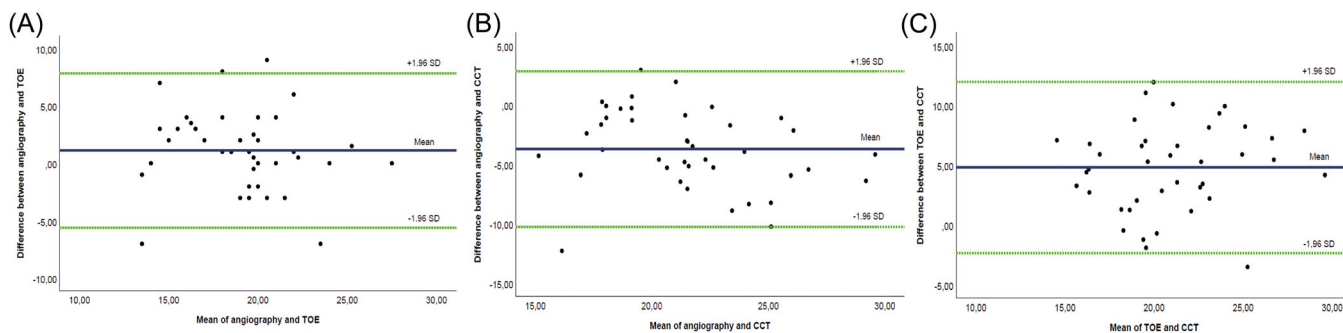
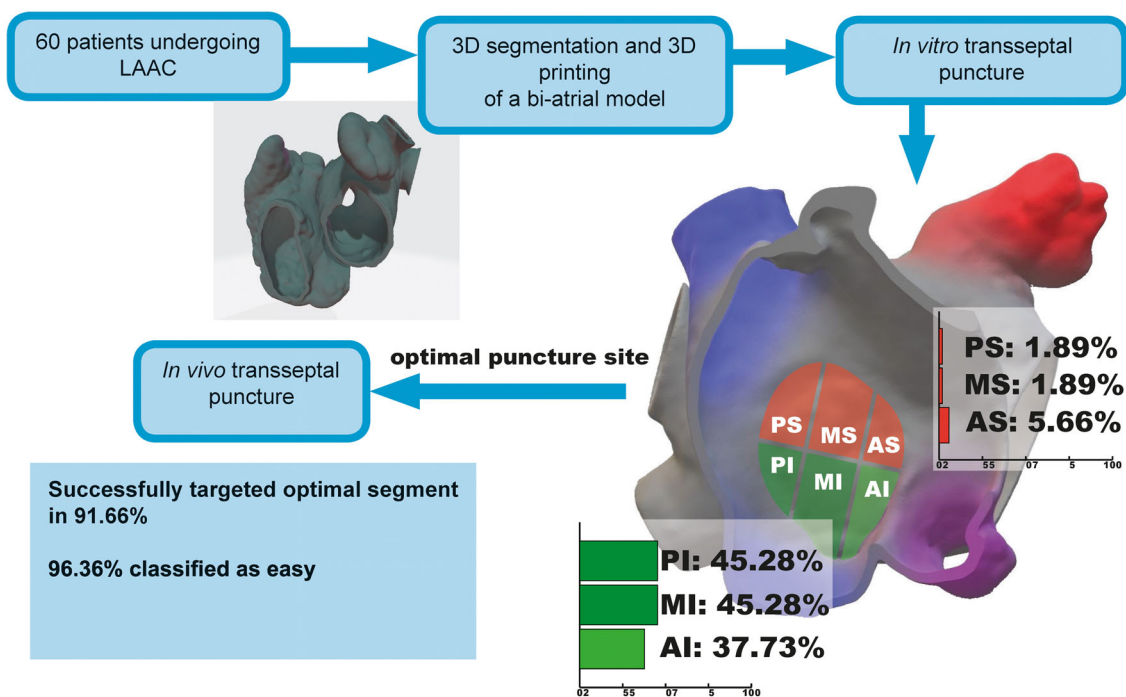


FIGURE 7 Bland–Altman plots comparing angiography and TOE (A), angiography and CCT (B) and TOE and CCT (C). CCT, cardiac computed tomography; TOE, transoesophageal echocardiography. [Color figure can be viewed at [wileyonlinelibrary.com](https://onlinelibrary.wiley.com/doi/10.1002/ccd.30867)]

Transseptal puncture in left atrial appendage closure guided by 3D printing and multiplanar CT reconstruction



CENTRAL ILLUSTRATION 1 Study design. AI, antero-inferior; AS, antero-superior; LAAC, left atrial appendage closure; MI, mid-inferior; MS, mid-superior; PI, postero-inferior; PS, postero-superior. [Color figure can be viewed at [wileyonlinelibrary.com](https://onlinelibrary.wiley.com/doi/10.1002/ccd.30867)]

each category). However, it is interesting to note that an antero-inferior location was recommended and achieved during the procedure in 38% of patients (Central illustration 1).

Developing noncoronary interventional procedures requires complex imaging technologies to better understand cardiac anatomy and its relationship to pathological conditions. 3DP is an emerging technology suitable for a wide range of interventional procedures.¹² Given the growing interest in 3D technologies as part of personalized medicine, our feasibility study tested the utility of 3D printing in achieving precise TSP in patients undergoing LAAC.

Several reports have been published on the benefits of 3D printing of the LAA or LA (as a single atrial model) for LAAC, most of which focused on device sizing. In 2016, Liu et al.¹³ reported the feasibility of using 3D-printed LA models based on real-time 3D TOE data to predict peri-device leaks and procedure-related difficulties. A study confirming that 3D printed models of the LAA can be generated from 3D TOE volumetric datasets was published by Song et al.¹⁴ Obasare et al.¹⁵ prospectively used 3D-printed left atrial models derived from CCT for preprocedural planning in a group of 14 patients to demonstrate its superiority over TOE alone in reducing procedure time and risk of PDL. Conti et al.¹⁶ reported that using a

3D-printed LA model based on CCT prevented underestimation of occluder size. Similar data regarding the advantage of using 3DP models for device sizing were reported by Fan et al.¹⁷ in a retrospective analysis. However, for TSP planning, the bi-atrial model has significant advantages over 3D-printing the LA and LAA alone: it allows mimicking similar manipulations with the delivery sheath in the atria during the actual procedure. The right atrium's presence significantly influences the delivery sheath's entry position in the LA, preventing TSPs in locations that would not be accessible in an actual procedure. To the best of our knowledge, our study is the first to demonstrate the feasibility of creating bi-atrial models suitable for in vitro TSP simulation as a new option to facilitate the safety and effectiveness of LAAC procedures. The biatrial model is easy to create, and the success rate of performing TSP at the target site exceeds 90%, with almost equal prevalence of echocardiographic guidance modalities (ICE and TOE).

To facilitate device deployment, TSP should be performed to maximize alignment of the delivery sheath axis with the axis of the proximal segment of the LAA. In line with previous recommendations and findings, puncture sites in the cranial part of the FO should be avoided, as their prevalence among optimal sites was less than 10% (with the adjacent inferior segment being optimal in all cases). On the other hand, the posteroinferior TSP considered a universal optimal puncture site,¹⁸ is only beneficial in less than half of the cases. In the other half of cases, the antero-inferior or mid-inferior TSP provided better alignment of the delivery sheath with the LAA axis. The information on the optimal TSP location obtained preprocedurally with a targeted TSP during the procedure could be of great importance for inexperienced or low-volume operators but could also facilitate the procedure for high-volume operators.

As 3D printing is time-consuming and limited in availability, we attempted to find a CCT-derived 2D parameter suitable for predicting an optimal TSP location. Our observations have indicated that the angle between the LAA ostium and the mitral annulus differs significantly when comparing optimal anterior and posterior locations. A value significantly higher or lower than 100° suggests that the TSP should be performed in the posterior or anterior position, respectively.

Notably, all three complications occurred in patients with TSP performed in an optimal location. Most TSPs were carried out at the optimal site; however, the cause of complications was not the incorrect TSP with subsequent difficult manipulations within the LA and LAA but an incorrect LZ measurement or an unusual LAA morphology. LZ measurement and device sizing were performed according to the operator's practice (CT, TOE, or angiography), and 3D-printed models were not used for device sizing. In our opinion, current practice using multimodality imaging, especially when CT is included, provides satisfactory results regarding device sizing. However, including the biatrial 3DP model in preprocedural planning provides another tool for TSP planning besides 2D CT, TOE, ICE, or angiography.

In terms of preprocedural in vitro simulation modalities, virtual reality (VR) appears to have the potential to replace 3DP in the future due to its greater availability, lower cost and reduced manpower requirements. In 2018, James and colleagues reported data on the

feasibility of VR guidance for TSP using a phantom containing a 3D-printed heart model.¹⁹ More recently, a group led by Tejman-Yarden published intriguing data on the utility of VR for device sizing. They reported that the maximum diameter of the LZ measured by VR correlated better with the final device selection compared to CCT and TOE.²⁰ However, the role of VR also needs to be tested against the standard approach.

Another possibility to facilitate the procedure is the utilization of a steerable transseptal sheath.²¹ Bending or deflecting the sheath could potentially help to compensate for "low" or "high" TSP; however, the anteroposterior orientation, which is determined by the anteroposterior location of the TSP, remains unaffected. Therefore, even with a steerable sheath, selecting an optimal TSP location remains one of the critical steps of the procedure.

As mentioned above, 3D printing was not applied for sizing as there are still some concerns about this concept (mainly due to the limitations of the material in mimicking natural tissue). Our approach is to calculate the average LZ diameter based on the CCT circumference measurements. When analysing this set, we also observed significant differences between the three different ways of measuring the LZ, with the values obtained by CCT analysis being the largest. These results are fully consistent with those reported elsewhere.^{22,23}

5 | STUDY LIMITATIONS

Our study has several limitations. The most important may be the lack of a control group due to the feasibility of this project. Another limitation is the relatively small number of subjects. Only large-scale controlled trials could prove the clinical usefulness of 3D printing. The vast majority of procedures were performed using the Amulet device. This is due to the operator's preference and is one of the limitations, as the preprocedural planning is different for the other devices. CT scans were not performed on the day of the procedure; therefore, the LA filling status could differ from the conditions during the procedure. Due to the routine protocol settings of the participating centers, CCT scans were performed in the end-diastolic phase, which underestimates LA volume and could potentially be a source of error.²⁴ As our study focused on TSP and not sizing, it is unlikely that the filling volume could significantly affect the results. The filling status or the phase in which the CT scans were performed could significantly affect the LA volume but not the LAA shape. Finally, the materials available for 3D printing cannot fully simulate a natural tissue characteristic.

6 | CONCLUSIONS

TSP simulation using bi-atrial 3D printed models is feasible and may constitute another useful modality for preprocedural planning. Surprisingly, the optimal TSP is located anteriorly in more than one-third of patients. Measuring the angle between the LAA ostium and the mitral annulus could help to decide whether the puncture site should be posterior or anterior.

ACKNOWLEDGMENTS

This study was supported by the project National Institute for Research of Metabolic and Cardiovascular Diseases "CarDia" (Programme EXCELES, ID Project No. LX22NPO5104), funded by the European Union—Next Generation EU. Partly the manuscript was co-funded also by the Charles University Research Program "Cooperatio Cardiovascular Sciences."

CONFLICT OF INTEREST STATEMENT

The authors declare no conflict of interest.

DATA AVAILABILITY STATEMENT

The data that support the findings of this study are available on request from the corresponding author. The data are not publicly available due to privacy or ethical restrictions.

ORCID

Marek Hozman  <http://orcid.org/0000-0003-4111-4218>

Pavel Osmancik  <http://orcid.org/0000-0003-0482-4448>

REFERENCES

- Benjamin EJ, Muntner P, Alonso A, et al. Heart disease and stroke statistics-2019 update: a report from the American Heart Association. *Circulation*. 2019;139:e56-e528.
- Sankaranarayanan R, Kirkwood G, Visweswariah R, Fox D. How does chronic atrial fibrillation influence mortality in the modern treatment era? *Curr Cardiol Rev*. 2015;11:190-198.
- Wolf PA, Abbott RD, Kannel WB. Atrial fibrillation as an independent risk factor for stroke: the framingham study. *Stroke*. 1991;22:983-988.
- McGrath ER, Kapral MK, Fang J, et al. Association of atrial fibrillation with mortality and disability after ischemic stroke. *Neurology*. 2013;81:825-832.
- Blackshear JL, Odell JA. Appendage obliteration to reduce stroke in cardiac surgical patients with atrial fibrillation. *Ann Thorac Surg*. 1996;61:755-759.
- Holmes DR, Reddy VY, Turi ZG, et al. Percutaneous closure of the left atrial appendage versus warfarin therapy for prevention of stroke in patients with atrial fibrillation: a randomised non-inferiority trial. *Lancet*. 2009;374:534-542.
- Holmes DR, Kar S, Price MJ, et al. Prospective randomized evaluation of the watchman left atrial appendage closure device in patients with atrial fibrillation versus long-term warfarin therapy. *JACC*. 2014;64:1-12.
- Osmancik P, Herman D, Neuzil P, et al. Left atrial appendage closure versus direct oral anticoagulants in high-risk patients with atrial fibrillation. *JACC*. 2020;75:3122-3135.
- Otton JM, Spina R, Sulas R, et al. Left atrial appendage closure guided by personalized 3D-printed cardiac reconstruction. *JACC Cardiovasc Interv*. 2015;8:1004-1006.
- Tarabanis C, Klapholz J, Zahid S, Jankelson L. A systematic review of the use of 3D printing in left atrial appendage occlusion procedures. *J Cardiovasc Electrophysiol*. 2022;33:2367-2374.
- Glikson M, Rafael W, Gerhard H, et al. EHRA/EAPCI expert consensus statement on catheter-based left atrial appendage occlusion—an update. *EuroIntervention*. 2020;15:1133-1180.
- Lindquist EM, Gosnell JM, Khan SK, et al. 3D printing in cardiology: a review of applications and roles for advanced cardiac imaging. *Ann 3D Print Med*. 2021;4:100034.
- Liu P, Liu R, Zhang Y, Liu Y, Tang X, Cheng Y. The value of 3D printing models of left atrial appendage using real-time 3D transesophageal echocardiographic data in left atrial appendage occlusion: applications toward an era of truly personalized medicine. *Cardiology*. 2016;135:255-261.
- Song H, Zhou Q, Zhang L, et al. Evaluating the morphology of the left atrial appendage by a transesophageal echocardiographic 3-dimensional printed model. *Medicine*. 2017;96:e7865.
- Obasare E, Mainigi SK, Morris DL, et al. CT based 3D printing is superior to transesophageal echocardiography for pre-procedure planning in left atrial appendage device closure. *Int J Cardiovasc Imaging*. 2018;34:821-831.
- Conti M, Marconi S, Muscogiuri G, et al. Left atrial appendage closure guided by 3D computed tomography printing technology: a case control study. *J Cardiovasc Comput Tomogr*. 2019;13:336-339.
- Fan Y, Yang F, Cheung GS-H, et al. Device sizing guided by echocardiography-based three-dimensional printing is associated with superior outcome after percutaneous left atrial appendage occlusion. *J Am Soc Echocardiogr*. 2019;32:708-719.
- Bergmann MW, Landmesser U. Left atrial appendage closure for stroke prevention in non-valvular atrial fibrillation: rationale, devices in clinical development and insights into implantation techniques. *EuroIntervention*. 2014;10:497-504.
- James RC, Monsky WL, Jorgensen NW, Seslar SP. Virtual-reality guided versus fluoroscopy-guided transeptal puncture in a cardiac phantom. *J Invasive Cardiol*. 2020;32:76-81.
- Tejman-Yarden S, Freidin D, Nagar N, et al. Virtual reality utilization for left atrial appendage occluder device size prediction. *Heliyon*. 2023;9:e14790.
- Kleinecke C, Gomez Monterrosas O, Scalone G, et al. First-in-human experience of left atrial appendage occlusion with the steerable FuStar sheath. *J Interv Cardiol*. 2018;31:532-537.
- Osmancik P, Herman D, Linkova H, Hozman M, Labos M. A comparison of cardiac computed tomography, transesophageal and intracardiac echocardiography, and fluoroscopy for planning left atrial appendage closure. *J Atr Fibrillation*. 2021;13:20200449.
- Rajwani A, Nelson AJ, Shirazi MG, et al. CT sizing for left atrial appendage closure is associated with favourable outcomes for procedural safety. *Eur Heart J Cardiovasc Imaging*. 2017;18:1361-1368.
- Fayad E, Boucebci S, Vesselle G, et al. Left atrial volume assessed by ECG-gated computed tomography: variations according to age, gender and time during the cardiac cycle. *Diagn Interv Imaging*. 2018;99:105-109.

How to cite this article: Hozman M, Herman D, Zemanek D, et al. Transseptal puncture in left atrial appendage closure guided by 3D printing and multiplanar CT reconstruction. *Catheter Cardiovasc Interv*. 2023;102:1331-1340. doi:10.1002/ccd.30867